SUPPLEMENTARY NOTE AND METHODS

Sidewall Oxide Effects on Spin-Torque and Magnetic-Field Induced Reversal Characteristics of Thin-Film Nanomagnets

O. Ozatay[†,*], P. G. Gowtham, K. W. Tan, J. C. Read, K. A. Mkhoyan, M. G. Thomas, G. D. Fuchs, P. M. Braganca, E. M. Ryan. K. V. Thadani, J. Silcox, D. C. Ralph, and R. A. Buhrman

Cornell University, Ithaca NY 14853-2501

Characterization of native oxides of Permalloy and their passivation with a thin Al layer

A full understanding of the effects of surface oxides on patterned ferromagnets necessitates a reliable identification of the oxide species present, including the interfacial chemistry with any potential capping layers deposited for the purpose of passivating the oxide formation. Permalloy (Py = $Ni_{81}Fe_{19}$), being a soft magnetic material with negligible anisotropy and low magnetostriction, has long been a very common material for spintronic devices. We have used x-ray photoemission spectroscopy (XPS) and electron energy loss spectroscopy (EELS) techniques to probe the surface chemistry of air-exposed Py and the interfacial interactions of Py with a thin AlO_x passivation layer.

Figure S1 shows a series of (a) Fe 2p and (b) Ni 2p high resolution XPS spectra (with the fitted peak structures) for the surface of an air-oxidized 5-nm-thick Py layer deposited on 200 nm of Cu and the surface of an identical Py layer that was coated with 1.5-nm-thick Al in-situ prior

[†] Present Address: Hitachi Global Storage Technologies, San Jose Research Center, San Jose, CA, 95135
* Corresponding author: Ozhan.Ozatay@hitachigst.com

to exposure to air. Since the $2p_{1/2}$ signal is usually not as strong as the $2p_{3/2}$ region, for the purpose of clarity we will discuss only the $2p_{3/2}$ peak structure but the corresponding peaks at $2p_{1/2}$ region can be observed in Fig. S1.

The Fe $2p_{3/2}$ region for the air-exposed Py sample can be fit with a four-peak structure with peak locations at 706.7 eV, 708.6 eV, 711 eV and 712.4 eV. The first three peaks indicate the presence of metallic Fe, FeO and Fe_2O_3 respectively[1]. We attribute the fourth peak to the possible presence of a surface FeOOH since the samples were air transferred from the growth to the XPS chamber. Using standard values[2] for the Fe $2p_{3/2}$ photoelectron attenuation length in FeO and Fe_2O_3 we estimate the total iron oxide thickness to be 7 ± 2 Å. The Fe peak structure for the AlO_x-passivated sample on the other hand can be fit using just 2 peaks at 706.9 and 711.2 eV, which correspond to metallic Fe and Fe_2O_3 components. The Al passivation layer successfully impedes the formation of any detectable FeO component and substantially lowers the amount of Fe_2O_3, with the Fe_2O_3 to Fe signal ratio being reduced by a factor of 4.

The Ni $2p_{3/2}$ spectrum of the air-exposed Py sample exhibits 4 peaks at 852.3 eV, 858.2 eV, 854.7 eV and 860.8 eV which we identify with metallic Ni, the Ni plasmon peak, NiO, and the oxide shake-up peaks respectively. Using the Ni $2p_{3/2}$ photoelectron attenuation length in NiO, we estimate the NiO thickness to be 13 ± 2 Å. The corresponding spectrum for the AlO_x-passivated sample shows no evidence for the presence of NiO or any hydroxides, just the 2-peak structure that is the signature of purely metallic Ni with its accompanying plasmon peak.

We conclude that either during the brief exposure of the Py to the background ambient, ~ 1×10^{7} Torr, in the vacuum chamber prior to the Al deposition or, more likely, during the subsequent oxidation of the Al layer there is a slight oxidation of the Fe atoms at the surface of the Py, but not of the Ni. This preferential behavior is consistent with the free energies of

formation for NiO and Fe_2O_3, -50.6 and -177.4 kcal/mol respectively, making Fe oxidation thermodynamically much more favorable than Ni oxidation[3].

Figure S2 shows a cross-sectional measurement of the elemental composition as a function of position at a Py/AlO_x interface, achieved using scanning transmission electron microscopy with electron energy loss spectroscopy (STEM-EELS). The thin film structure here is identical to that studied by XPS with the exception that an additional 5 nm of alumina was deposited on top of the AlO_x-passivated sample to protect the specimen surface during TEM specimen preparation. The (separately normalized) concentration profiles for O, Ni and Fe were obtained by integrating the intensity of the oxygen K edge, Ni $L_{2,3}$ edge and Fe $L_{2,3}$ edge EELS spectra. The inset of Fig. S2 shows a high-magnification annular-dark field (ADF) image of the Py/AlO_x interface. The ADF signal varies as $Z^{1.7}$ due to high-angle Rutherford scattering, and therefore yields a bright region for Py (Z_{Ni}=28, Z_{Fe}=26) in contrast to AlO_x (Z_{Al}=13).

The EELS investigation shows a sharp drop, from 75% to 25% within one nm, in the oxygen signal at the Py/AlO_x interface. The resolution of this measurement is limited by the cross-section projection of the surface roughness of the Py film, which was measured by atomic force microscopy to be ~1.2 nm. Thus the actual variation in the oxygen concentration is most likely sharper than this measurement resolution. The Ni concentration shows a more gradual but clear decrease across the interface. On the other hand, there is a local maximum in the Fe signal away from the AlO_x – Py interface and this Fe signal extends almost all the way to the surface of the AlO_x layer. This EELS measurement suggests that the Fe_2O_3 signal observed in the XPS measurement discussed above on the Al coated Py sample arises from a mixed oxide that forms during the Al oxidation process, and indicates that the Fe^{+3} ions are dispersed within the AlO_x

(nominally Al_2O_3) matrix, which should alter, and perhaps eliminate, their antiferromagnetic ordering.

SUPPLEMENTARY METHODS

The XPS spectra were acquired using a Surface Science Laboratories SSX-100 spectrometer equipped with a hemispherical energy analyzer with 0.6 eV energy resolution in an ultra-high-vacuum (UHV) chamber (~10^{-9} Torr). The locations of the metallic photoemission peaks for Fe $2p_{3/2}$ at 706.6 eV and Ni $2p_{3/2}$ at 852.3 eV, were used to calibrate each spectrum for spectrometer shifts. The XPS spectra were fit using the standard approach of first applying a Shirley background[4] and then using a 90% Gaussian and 10% Lorentzian line shape. Asymmetric tails were used for fitting metallic Ni and Fe peaks with asymmetry parameters of TS and TL being 0.4 and 70 for Fe $2p^{1/2}$, 0.5 and 100 for Fe $2p^{3/2}$, 0.3 and 40 for Ni $2p^{1/2}$ and 0 and 1 for Ni $2p^{3/2}$ peaks respectively in XPSpeak peak-fitting freeware[5]. The positive shifts in the binding energy for different oxidation states of Ni and Fe (which occur due to tighter binding of the core shell electrons in the ionic state) were used to identify the surface oxide components.

The oxide thicknesses were estimated considering the metal photoelectron attenuation effects in their corresponding oxides. For the case of NiO, this thickness t_{NiO} is given by[6]:

$$t_{NiO} = \lambda_{Ni,ox} \sin(\theta) Ln\left(\frac{\lambda_{Ni} C_{Ni}}{\lambda_{Ni,ox} C_{Ni,ox}} \frac{I_{NiO}}{I_{Ni}} + 1 \right)$$

where $\lambda_{Ni,ox}$ and λ_{Ni} are the Ni photoelectron attenuation lengths in NiO (13.4 Å) and in the metal (10 Å) respectively, $C_{Ni,ox}$ and C_{Ni} are the Ni concentrations in the NiO oxide layer (0.5) and in the metallic underlayer of permalloy (0.81) respectively, I_{NiO}/I_{Ni} is the oxide to metal peak intensity ratio acquired from the XPS spectrum (1.857) and θ is the relative angle between the

sample normal and the detector (~ 55˚). The same procedure was applied for iron oxides with attenuation lengths of ~16 Å in the oxide layer and 13.6 Å in the metallic underlayer.

For all STEM-EELS measurements a 2 Å diameter electron beam profile was used in spot-mode with 0.6 nm steps across the Py/AlO_x interface. These measurements were performed with the Cornell VG-HB501 STEM with a 100 keV accelerating voltage. The spatial drift rate is less than 0.3 nm/min and the energy drift rate is less than 0.03 eV/min. The energy resolution is better than 0.7 eV[7].

---

[1] *NIST X-ray Photoelectron Spectroscopy Database-Version 3.2* (National Institute of Standards and Technology, Gaithersburg, MD, 2003).

[2] *NIST Electron Effective-Attenuation-Length Database-version 1.0* (National Institute of Standards and Technology, Gaithersburg, MD, 2001).

[3] *CRC Handbook of Chemistry and Physics* (CRC Press, OH, 1986).

[4] Shirley, D. A. High-resolution x-ray photoemission spectrum of valence bands of gold. *Phys. Rev. B* **5**, 4709-4714 (1972).

[5] http://www.phy.cuhk.edu.hk/~surface/XPSPEAK/

[6] Tan, E. *Ph. D. Thesis* (Cornell University, Ithaca, NY 2005).

[7] Mkhoyan, K. A. *Ph. D. Thesis* (Cornell University, Ithaca, NY 2004).

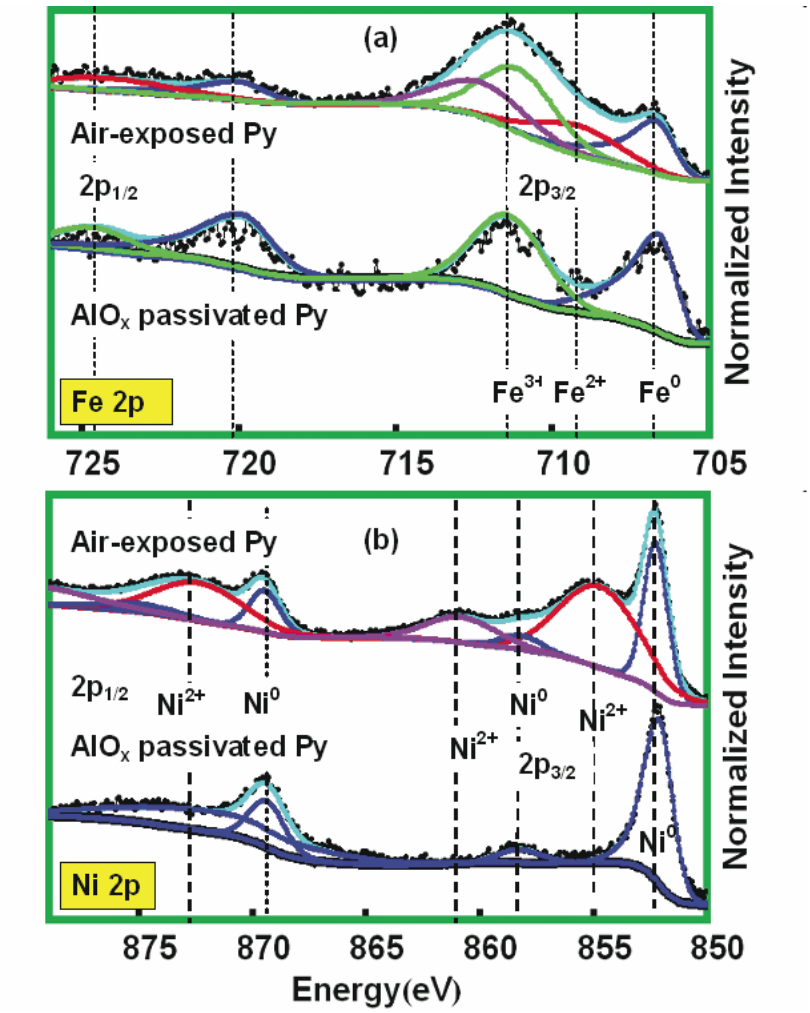

Supplementary Figure S1: High resolution X ray photoemission spectra of the air-exposed and Al-passivated Permalloy surface. **(a)** Fe 2p region and (**b)** Ni 2p region, measured on 50 nm thick Py films. The upper curves in each panel are for a Py surface exposed to air, and the lower curves are for a Py surface protected from oxidation by an AlO_x passivation layer.

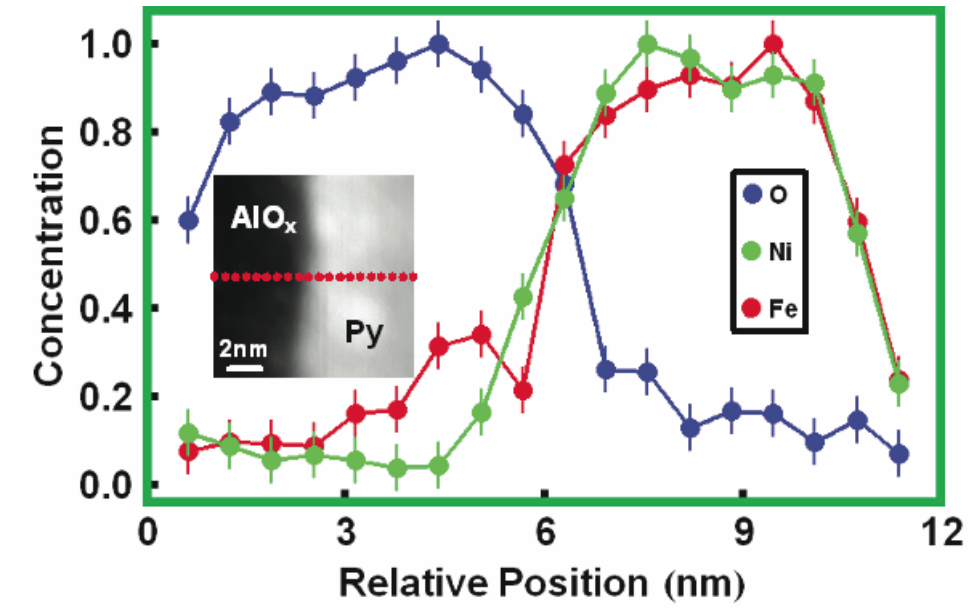

Supplementary Figure S2: Atomic-scale characterization of the Permalloy/AlO_x interface. Separately-normalized oxygen (blue dots), nickel (green dots) and iron (red dots) concentration profiles across a Py/AlO_x interface, prepared in the same way as the films measured with XPS, measured using STEM-EELS with 0.63 nm steps. The inset shows the corresponding high magnification ADF-STEM image with the red dotted line indicating the cut along which the EELS spectra were collected.